Poly(3-hydroxybutyrate-*co*-3-hydroxyvalerate)-Based Biocomposites Reinforced with Kenaf Fibers

Maurizio Avella,[1] Gordana Bogoeva-Gaceva,[2] Aleksandra Bužarovska,[2] Maria Emanuela Errico,[1] Gennaro Gentile,[1] Anita Grozdanov[2]

[1]*Institute of Chemistry and Technology of Polymers, National Research Council (ICTP-CNR), Via Campi Flegrei Comprensorio Olivetti, 80078 Pozzuoli (NA), Italy*
[2]*Faculty of Technology and Metallurgy, University Sts. Cyril and Methodius, 1000 Skopje, Republic of Macedonia*

Received 29 March 2006; accepted 16 December 2006
DOI 10.1002/app.26057
Published online 5 March 2007 in Wiley InterScience (www.interscience.wiley.com).

ABSTRACT: Biodegradable thermoplastic-based composites reinforced with kenaf fibers were prepared and characterized. Poly(3-hydroxybutyrate-*co*-3-hydroxyvalerate) (PHBV), produced by bacterial fermentation, was selected as polymeric matrix. To improve PHBV/fibers adhesion, low amount of a proper compatibilizing agent, obtained by grafting maleic anhydride onto PHBV, was added during matrix/fibers melt mixing (reactive blending). When compared with uncompatibilized composites, the presence of the compatibilizer induces a stronger interfacial adhesion and a more pronounced improvement of the mechanical properties. © 2007 Wiley Periodicals, Inc. J Appl Polym Sci 104: 3192–3200, 2007

Key words: PHBV; kenaf; composites; compatibilization; mechanical properties

INTRODUCTION

In the recent years, the use of renewable resources as chemical feedstock for the preparation of polymer-based materials has attracted an even growing attention because of the crisis of traditional petrochemical derived compounds and the increasing demand of environmental-friendly materials.[1,2] Among biodegradable polymeric materials from sustainable resources, polyhydroxyalkanoates (PHA) cover a wide market because of their performances that are similar and, in some cases, are better than those shown by conventional polymers. It was foreseen that PHA are potential candidates to replace over 50% of polymers and are now synthesized from oil and natural gas.[3] Among the PHA family, poly-3-hydroxybutyrate (PHB) is the most common polymer, but its potential industrial use has been limited by the narrow window of processability ($\Delta T \sim 20^{\circ}C$) and its poor mechanical properties. Nowadays, a large interest is devoted to PHB copolymers and, among them, to poly(3-hydroxybutyrate-*co*-3-hydroxyvalerate) (PHBV) with various relative amount of hydroxyvalerate units, because of an improved processability and better mechanical properties.[4] The drawbacks of PHBV are the still high cost compared to that of petroleum-based commodity plastics, and a relatively low impact resistance.[5,6]

It is well known that fiber reinforcement is a viable method to improve the mechanical properties of biodegradable plastics and to reduce the overall costs of the prepared materials.[7] However, conventional-reinforcing materials such as glass fiber, carbon fiber, and aramide fiber are not biodegradable thus preventing the realization of wholly ecosustainable composites. In this respect, natural plant-based lignocellulosic fibers are very attractive reinforcing materials.[8,9] Among lignocellulosic fibers, kenaf is attracting special attention because of its good mechanical properties (comparable to jute, sisal, and flax) and to its increasing cultivation in many developing and developed countries.[10] Although kenaf has been already tested as natural reinforcement for polyolefyns,[11,12] only a few studies[13,14] on its use for the preparation of biocomposites are reported in literature.

The key factor in the preparation of PHBV/kenaf composites is the compatibilization, because of their different surface chemistry. Lignocellulosic fibers are hydrophilic, whereas PHBV is hydrophobic. Therefore, compatibilization strategies have to be considered to optimize the effects of the reinforcement phase.[15]

Correspondence to: M. Avella (mave@ictp.cnr.it).
Contract grant sponsor: European Commission in the Sixth Framework Programme; contract grant number: Priority FP6-2002-INCO-WBC-1.
Contract grant sponsor: International Cooperation with Western Balkans Countries.
Contract grant sponsor: European Commission, Sixth Framework Programme, International Cooperation with Western Balkan Countries, Specific Targeted Research or Innovation Project; contract grant number: FP6-2002-INCO-WBC-509185.

The main goal of this work was the preparation and the characterization of new PHBV-based composites reinforced with kenaf fibers with particular attention to the promotion of a reactive interface between matrix and filler and to the influence of the improved interfacial adhesion on the final composite properties. Concerning the compatibilization strategy, a proper coupling agent (CA) was synthesized by grafting maleic anhydride (MA) onto PHBV backbone. Then, composites were prepared by reactive blending and their morphological, thermal, and mechanical properties were investigated. The influence of the CA on the final properties was studied by comparing uncompatibilized and compatibilized composite performances.

EXPERIMENTAL

Materials

Kenaf fibers, average length 5.1 mm and average diameter 21 μm, were kindly supplied by Kenaf Eco Fibers Italia S.p.A. (Guastalla-Italy).

PHBV, hydroxyvalerate unit content 13 mol %, was supplied by Biomer (Krailling-Germany).

MA, dibenzoylperoxide (DBPO), and chloroform were supplied by Sigma-Aldrich (Steinheim-Germany) and were used as received.

CA preparation

About 48.5 g (47.5 g; 46.5 g) of PHBV were mixed for 3 min in the Brabender-like apparatus at 170°C, and then 1.5 g (2.5 g; 3.5 g) of MA and 0.75 g of DBPO were added. The mixture was blended at 170°C for further 5 min, increasing progressively the mixing rate up to 32 rpm. Finally, the obtained material was dried under vacuum at 100°C to remove the unreacted MA. The obtained CA was coded as CA3 (CA5; CA7).

PHBV-based composites preparation

PHBV-kenaf composites were prepared by melt mixing in a Brabender-like apparatus (Rheocord EC of HAAKE, NJ). Two kinds of composites were prepared through the following procedures.

Uncompatibilized composites were obtained by mixing 40 g (35 g) of PHBV at 170°C for 3 min. Then, 10 g (15 g) of dry kenaf fibers was added and the mixture was blended at 170°C for further 7 min, increasing progressively the mixing speed up to 32 rpm. Corresponding sample is coded as PHBV/K 80/20 (PHBV/K 70/30).

Compatibilized PHBV-kenaf composites were prepared as follows: 37.5 g (32.5 g) of PHBV and 2.5 g of CA3 were mixed in the Brabender-like apparatus for 3 min. Thereafter, 10 g (15 g) of dry kenaf fibers was added and the mixture was blended at 170°C for further 7 min, increasing progressively the mixing rate up to 32 rpm. Corresponding sample is coded as PHBV/CA/K 75/5/20 (PHBV/CA/K 65/5/30).

Finally, the materials were compression molded at 170°C for 5 min (10 ton) to obtain 65 mm × 65 mm × 3.5 mm specimens.

Techniques

Fourier transformed infrared analysis

FTIR (Fourier transformed infrared) spectra of neat PHBV and PHBV grafted with MA were recorded at room temperature with a PerkinElmer Paragon 2000 Fourier transform infrared spectrometer (Switzerland), using 64 scans and a resolution of 2 cm^{-1}. The samples were dissolved in chloroform, and then casted on KBr disks.

Viscosimetric analysis

The viscosimetric molecular weight of neat PHBV, PHBV processed at 170°C for 10 min, and PHBV grafted with MA (CA) was determined by means of viscosimetric analysis in chloroform at 25°C, using the Mark-Houwink-Sakurada relationship[16]:

$$[\eta] = KM_w^{\alpha} \quad (1)$$

where $K = 0.012$ mL g^{-1} and $\alpha = 0.77$.[6,17]

Morphological analysis

The surface analysis was performed by using a scanning electron microscope (SEM), Cambridge Stereoscan microscope model 440, on cryogenically fractured surfaces of the composite samples. Before the observation, the specimens were metallized with a gold/palladium coating.

Calorimetric analysis

Thermal properties were measured by using a differential scanning calorimeter Mettler DSC-30. Dry nitrogen gas with a flow rate of 200 mL min^{-1} was purged through the cell during measurements. Samples were heated from 25 to 175°C at a scanning rate of 10°C min^{-1} (I run), cooled to 0°C at 10°C min^{-1} (cooling run), and then reheated to 185°C at 10°C min^{-1} (II run). Crystallization temperature values (T_c) were measured as the maximum of the exothermic peaks of DSC traces during the cooling scan. Melting temperature values (T_m) were measured as the minima of the endothermic peaks of DSC traces during the II run. Crystalline fractions (X_c) were calculated by integra-

tion of the crystallization exotherms ($X_{c,c}$) during the cooling run and by integration of the melting endotherms ($X_{c,h}$) during the II run, using the literature data for the PHBV melting enthalpy of 109 J g^{-1}.[18]

Thermogravimetric analysis

The thermal stability of the samples was measured by means of TGA with a PerkinElmer Pyris Diamond Thermogravimetric/Differential Thermal Analyzer, recording the weight loss as a function of the temperature. Samples were heated from 40 to 700°C at a scanning rate of 10°C min^{-1} in nitrogen atmosphere. Degradation temperature values (T_d) were evaluated as the temperatures corresponding to the maximum rate of weight loss.

Dynamic-mechanical analysis

Dynamic-mechanical data were collected at 1 Hz and at a heating rate of 3°C min^{-1} from −50 to 120°C under nitrogen flow with a PerkinElmer Pyris Diamond Dynamic Mechanical Analyzer. The experiments were performed in bending mode on samples 20 mm long, 14 mm wide, and 3.5 mm thick.

Mechanical analysis

The flexural strength and the flexural modulus were measured in three-points bending mode using an Instron machine (model 5564), at a cross-head speed of 1 mm min^{-1} and at room temperature. Test specimens were 3.5 mm thick, 6.0 mm wide, and 60 mm long. The test span was 48.0 mm. For each sample, 10 specimens were tested and the average values of the flexural strength and modulus were calculated.

Fracture tests were carried out with a Charpy Ceast Resil Impactor equipped with a DAS 4000 Acquisition System at an impact speed of 1 m s^{-1}. Samples with a notch depth to width ratio of 0.3 and a span length of 48.0 mm, 6.0 mm wide, 3.5 mm thick, and 60 mm long, were fractured at room temperature (ASTM D256). The relative curves of energy and load were recorded. For each sample, 10 specimens were fractured and the average values of the resilience were calculated.

RESULTS AND DISCUSSION

CA preparation and characterization

To increase the compatibilization between PHBV and kenaf fibers a proper CA was prepared. In particular, PHBV was modified by grafting different amount of MA (3, 5, and 7 wt %) onto polymeric backbone through the thermal decomposition of DBPO, according to Scheme 1. The insertion of MA mainly occurs onto hydroxybutyrate units, probably due to statistical, steric, and chemical effects. In fact, the relative higher amount of hydroxybutyrate units with respect to that of hydroxyvalerate (13 mol %) renders the first more available to MA grafting. Concerning the steric effect, it must be underlined that the ethyl group on the β-carbon could also prevent the grafting of MA onto hydroxyvalerate units because of its higher hindrance. Finally, this ethyl group is responsible for a reduced acidity and then a reduced availability of the hydrogen atom bonded to the β-carbon to the radical attack.

The grafting reaction was performed in bulk. This choice permits to reduce the overall environmental impact of the process with respect to a possible PHBV chemical modification strategy carried out in solution.[19,20]

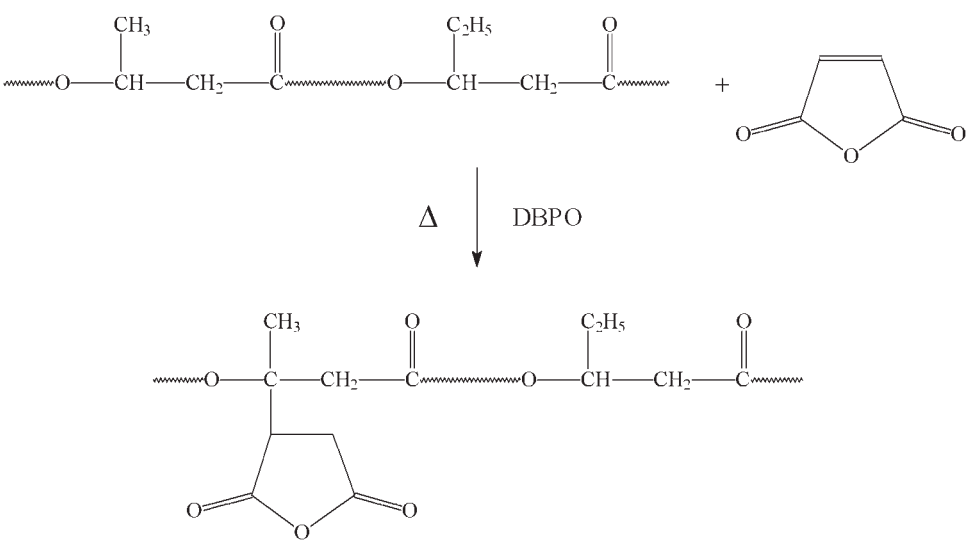

Scheme 1 Reaction scheme between PHBV and maleic anhydride in presence of dibenzoylperoxide (DBPO).

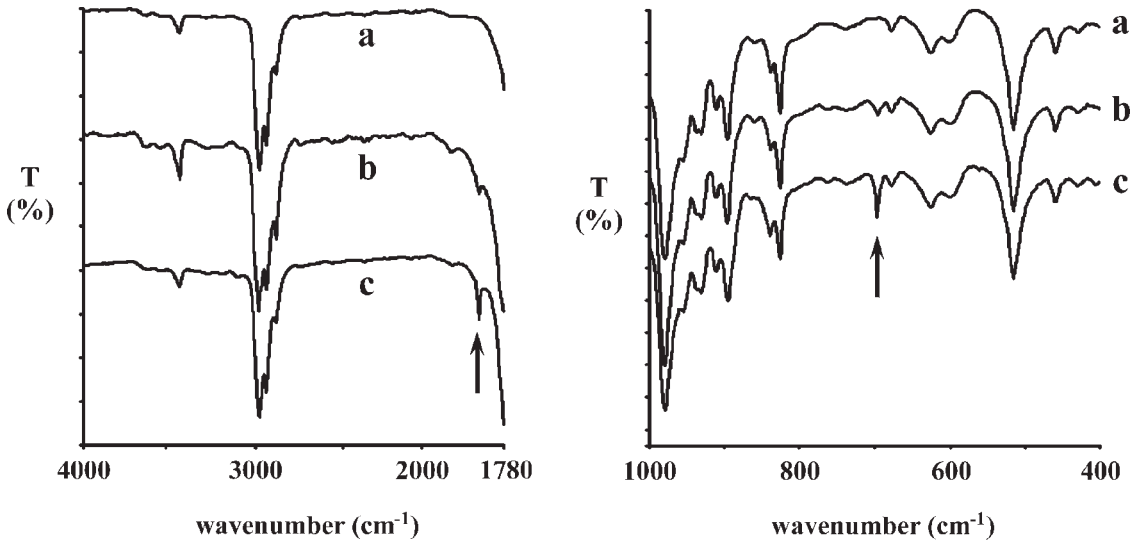

Figure 1 FTIR spectra of (a) neat PHBV; (b) PHBV grafted with 3% maleic anhydride (CA3); (c) PHBV grafted with 3% maleic anhydride (CA7).

The grafting reaction of MA was monitored by FTIR analysis. In Figure 1, different regions of FTIR spectra of neat PHBV and PHBV grafted with the lowest and the highest content of MA (CA3 and CA7) are reported. As it can be observed, new absorption bands centered at 1850 and 690 cm^{-1}, whose intensities are a function of MA amount, appear in the spectra of modified PHBV. These bands can be attributed to the asymmetric stretching of the MA carbonyl group and to the bending of the CH group of grafted anhydride ring, respectively, thus confirming the occurred reaction.

To evaluate the effects of both the process and the grafting reaction on the possible PHBV degradation, viscosimetric analysis was performed on neat PHBV, PHBV processed at 170°C for 10 min, and PHBV grafted with different amount of MA (CA). In Table I, the results of the viscosimetric analysis are reported. As it is shown, the process conditions are responsible for a slight decrease of the PHBV molecular weight. Concerning the grafting reactions, PHBV degradation was observed as a function of the MA content. This result can be explained taking into account that higher the MA amount, higher radical molecule concentration that could induce macromolecular scission, thus significantly reducing the PHBV molecular weight.

As a matter of fact, PHBV modified with 3% of MA (CA3) was selected as CA for the preparation of the compatibilized composites.

Composite preparation and morphology

PHBV-based composites were prepared by reactive blending. As it is reported in literature, this preparation methodology is an effective strategy to promote the compatibilization of PHA with different materials.[5,21,22] In particular, 5 wt % of the reactive CA3, obtained as described earlier, was added during the mixing of PHBV and kenaf fibers. In fact, it is well known that reactions between MA groups grafted onto polymeric backbones and hydroxyl groups of cellulose fibers can occur during the mixing, enhancing the compatibilization among composite components.[15,23] A compatibilization strategy based on PHBV modification was preferred to the chemical modification of cellulose fibers that consists on the esterification of the cellulose fraction of the fibers by using dicarboxyl acid anhydrides such as succinic anhydride (SA) and MA. The esterification reaction is illustrated in Scheme 2.[24] Nevertheless, it has been widely pointed out that exchange reactions may occur during the melt mixing of polyesters in presence of species containing reactive end-groups, such as hydroxyl, carboxyl, and amine groups.[25,26] As a matter of fact, carboxyl end-groups bonded to cellulose fibers (Scheme 2) could attack the inner ester groups of PHBV, yielding random scission reactions. As a consequence, a drastic decrease of PHBV molecular weight could occur with a decrease of mechanical strength, chemical, and thermal resistance of the polymer.[27–29]

TABLE I
Molecular Weight of Neat PHBV, Processed, and Modified PHBV

Samples	M_W (Da)
PHBV neat	123,000
PHBV processed	116,000
CA3	112,000
CA5	96,000
CA7	77,000

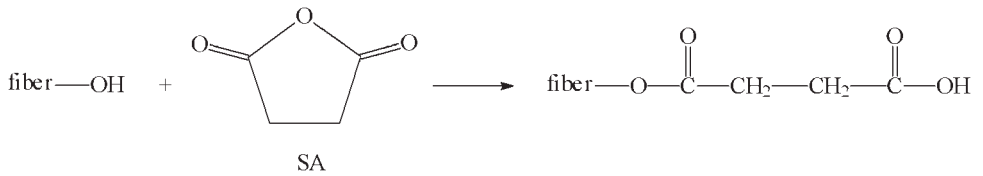

Scheme 2 Reaction scheme between cellulose fibers and succinic anhydride (SA).

To evaluate the influence of the CA on morphology and final properties of composites, uncompatibilized materials were also prepared. Morphological analysis was performed on cryogenically fractured surfaces of uncompatibilized and compatibilized materials. As an example, in Figure 2, micrographs of composites containing 20 wt % of kenaf fibers are reported. Concerning the PHBV/K 80/20 composite [Fig. 2(A)], kenaf fibers appear not wholly embebbed into PHBV. Moreover, the fibers are strongly damaged and some debonding phenomena are evident, thus indicating a poor fiber–polymer adhesion. Instead, as it can be observed from Figure 2(B), a significant enhancement of the adhesion level between the fibers and the matrix can be remarked for the compatibilized composite PHBV/CA/K 75/5/20. In fact, the fibers are well welded to PHBV and the absence of voids indicates that no debonding phenomena occur. This result permits to assess that reactive blending allows a significant improvement of the fiber–polymer interfacial adhesion.

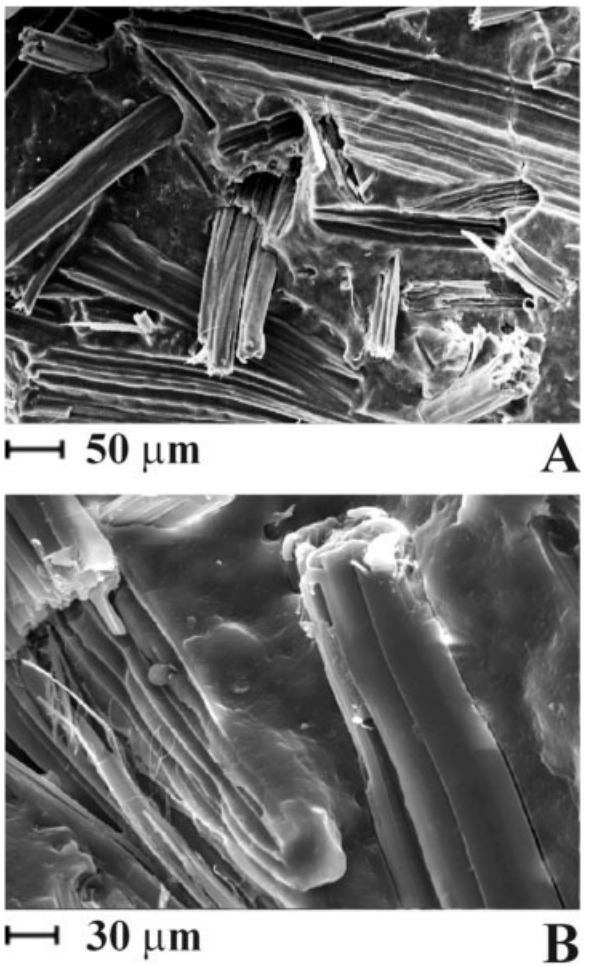

Figure 2 Scanning electron micrographs of (A) uncompatibilized PHBV/K 80/20 composite; (B) compatibilized PHBV/CA/K 75/5/20 composite.

Composite characterization

Thermal properties

Table II summarizes thermal data obtained through DSC analysis, of neat PHBV and PHBV-based composites. DSC thermograms show an endothermic double peak both during I and II run. This double peak can be probably attributed to recrystallization phenomena occurring during melting.[30] The related melting temperature values, measured in II run, are reported in Table II as T_{m1} and T_{m2}, respectively. Although T_{m2} seems to be not influenced by the presence of kenaf fibers, either for uncompatibilized or for compatibilized composites, T_{m1} values slightly increase by the addition of kenaf fibers. Moreover, during the nonisothermal crystallization process (cooling run), the DSC traces show a single exothermic peak, whose maximum (T_c) seems to slightly decrease with respect to neat PHBV. Both these findings can be explained by considering that kenaf/PHBV interactions can induce a slight delay either into the melting or into the crystallization process, as it has also been found for other PHA-based composites filled with cellulose fibers.[31]

The thermal degradation of neat components (kenaf, PHBV) and composites has been investigated in terms of weight loss by thermogravimetric analysis carried out under nitrogen atmosphere. TGA data are shown in Figure 3(A), in which the residual weight is

TABLE II
Thermal Properties of Neat PHBV and PHBV/Kenaf Composites

Samples	T_c (°C)	T_{m1} (°C)	T_{m2} (°C)	$X_{c,h}$ (%)
PHBV neat	100	147	157	39
PHBV/K 80/20	98	150	158	38
PHBV/K 70/30	97	151	157	38
PHBV/CA/K 75/5/20	98	151	158	39
PHBV/CA/K 65/5/30	96	152	157	37

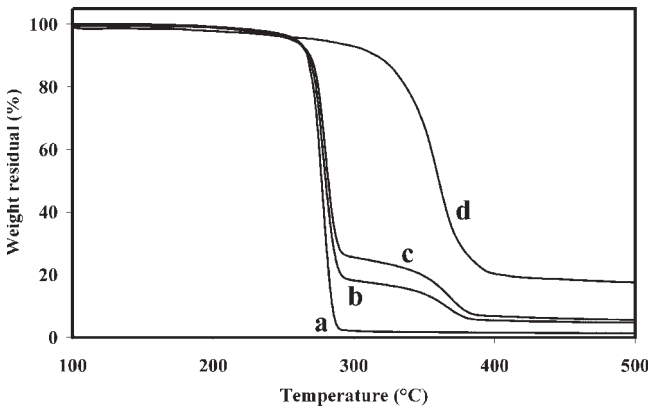

Figure 3 Results of the thermogravimetric analysis under N_2 flow: residual weight of (a) neat PHBV; (b) PHBV/K 80/20 and PHBV/CA/K 75/5/20; (c) PHBV/K 70/30 and PHBV/CA/K 65/5/30; (d) kenaf fibers.

presented in graphical form, as a function of temperature, for kenaf, PHBV, and PHBV/kenaf composites. In Table III, the degradation temperature values (T_d), calculated as the maximum of the degradation rate, and the residual weight at 500°C are reported. It can be observed that for both kenaf and PHBV, the thermal degradation occurs in a single step, whose maximum rates are centered at 277 and 348°C, respectively. On the other hand, the composite degradation phenomenon is a two-step process. The first step, whose maximum in the degradation rate is between 278 and 280°C, can be attributed to the thermal decomposition of the matrix, whereas the second step, centered at higher temperatures, is related to the thermal degradation of kenaf fibers. Concerning the residual weight at 500°C, whose values are reported in Table III, it can be remarked that kenaf shows a very high residual weight, about 17%, in agreement with data reported in literature for cellulose fibers.[32] As a consequence, the residual weight at 500°C is higher for composites with the highest kenaf amount (PHBV/K 70/30 and PHBV/CA/K 65/5/30) with respect to that recorded for composites containing 20 wt % of kenaf fibers (PHBV/K 80/20 and PHBV/CA/K 75/5/30). Finally, the presence of the CA does not affect the thermal degradation process. In fact, the weight residual curves of the compatibilized and uncompatibilized materials containing the same amount of fibers are overlapped.

TABLE III
Thermogravimetric Data of Neat PHBV and PHBV/Kenaf Composites: Degradation Temperature (T_d) and Residual Weight at 500°C

Samples	T_d (°C)	Weight residual at 500°C (%)
PHBV neat	277	1.4
Kenaf	348	17.2
PHBV/K 80/20	278	4.5
PHBV/K 70/30	280	5.6
PHBV/CA/K 75/5/20	279	4.4
PHBV/CA/K 65/5/30	280	5.6

Thermomechanical and mechanical properties

DMA results are illustrated in Figure 4(A–C) and summarized in Table IV. In particular, it can be

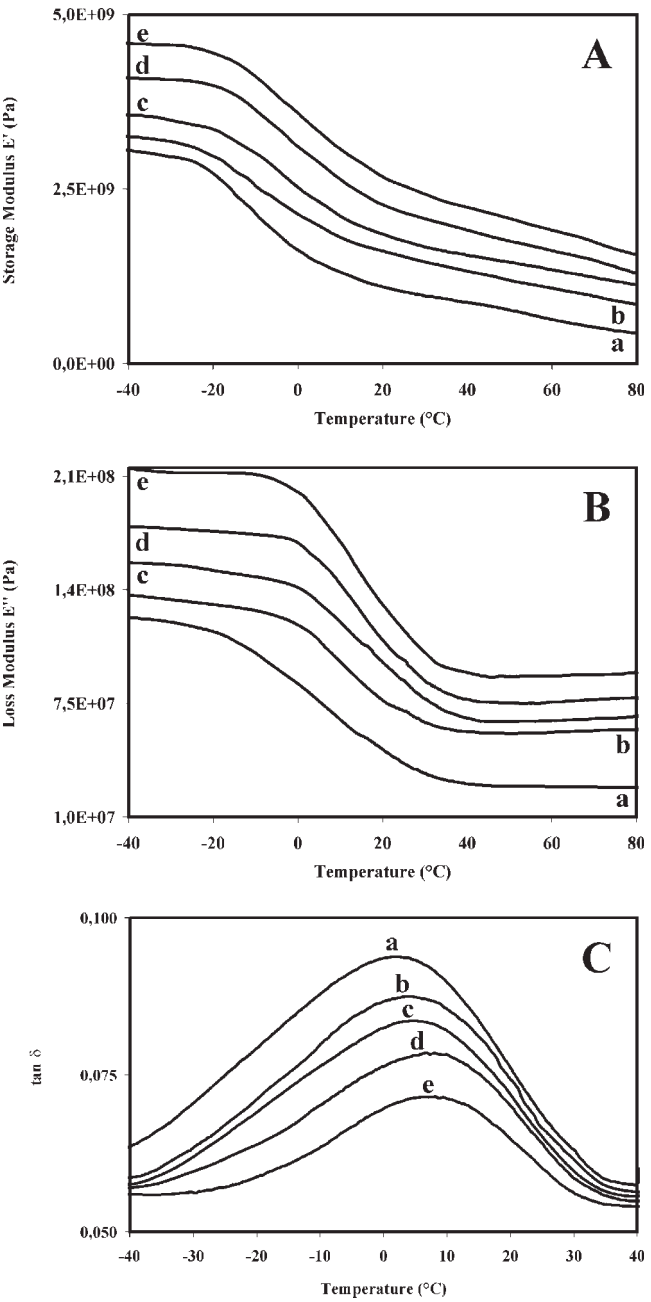

Figure 4 Results of the dynamic mechanical analysis: (A) storage modulus E', (B) loss modulus E'', and (C) tan δ for the samples: (a) neat PHBV; (b) PHBV/K 80/20; (c) PHBV/K 70/30; d) PHBV/CA/K 75/5/20; (e) PHBV/CA/K 65/5/30.

TABLE IV
Dynamic-Mechanical Results of Neat PHBV and PHBV/Kenaf Composites: Storage Modulus (E') and Loss Modulus (E') at −40 and +40°C, and Glass Transition Temperature (T_g)

Samples	$E'_{-40°C}$ (MPa)	$E'_{+40°C}$ (MPa)	$E''_{-40°C}$ (MPa)	$E''_{+40°C}$ (MPa)	T_g (°C)
PHBV neat	3062	879	124	29	2.9
PHBV/K 80/20	3237	1347	137	59	4.7
PHBV/K 70/30	3554	1558	156	67	4.7
PHBV/CA/K 75/5/20	4091	1867	176	77	8.6
PHBV/CA/K 65/5/30	4584	2205	209	92	8.5

observed that both the storage modulus (E') and the loss modulus (E'') increase with the fiber contents. Furthermore, it can be remarked that the compatibilized materials [PHBV/CA/K 75/5/20 and 65/5/30, curves *d* and *e*, respectively, in Fig. 4(A,B)] show higher storage and loss modulus values with respect to the uncompatibilized composites and neat PHBV in all the investigated range of temperature.

Moreover, the glass transition temperature (T_g) values, calculated as the temperature corresponding to the maximum of tan δ [Fig. 4(C)] are also influenced by kenaf content and compatibilization procedure. In fact, uncompatibilized composites [curves *b* and *c* in Fig. 4(C)] show T_g values slightly higher than neat PHBV, whereas a more pronounced increase is recorded for the compatibilized composite samples [curves *d* and *e* in Fig. 4(C)], up to 5.7°C (Table IV).

The more pronounced increase of the storage and loss modulus and the T_g values can be explained considering that the compatibilization procedure is able to induce an improved fiber-matrix adhesion with respect the uncompatibilized materials, in agreement with results obtained by morphological analysis. To confirm this assumption, the adhesion parameter A of the fiber-matrix interface was also evaluated.[33,34] The parameter A is defined by the following equation[35]:

$$A = \frac{1}{1 - V_F} \frac{\tan \delta_C(T)}{\tan \delta_M(T)} - 1 \qquad (2)$$

where V_F is the volume fraction of the filler in the composite, and tan $\delta_C(T)$ and tan $\delta_M(T)$ are the values of tan δ, measured at the temperature T, of the composite and the pure matrix, respectively.

It is to be remarked that the adhesion parameter A is inversely correlated with the adhesion level between the composite components, that is, lower A corresponds to higher fiber-matrix interactions.

The adhesion parameter A versus temperature in the temperature range below the glass transition temperature of neat matrix is presented in Figure 5. As it can be observed, the adhesion level is a function of the fiber content. In fact, for both uncompatibilized (curves *a* and *b*) and compatibilized (curves *c* and *d*) composites, lower kenaf content induces stronger interactions between matrix and fibers. This phenomenon can be explained by considering that at 20 wt % of kenaf contents the interactions fiber/matrix are already maximized, because of a sort of saturation of the polymeric phase that is not longer able to promote higher adhesion level with further fibers.

Moreover, the adhesion parameter curves both for lower and higher kenaf amount of compatibilized samples lay below those of the uncompatibilized samples in all the graphed temperature range. It is also to be remarked that the gap of the adhesion parameter between compatibilized composites (Fig. 5, curves *c* and *d*) is halved with respect to the extent of the gap between uncompatibilized composites (Fig. 5, curves *a* and *b*). As a matter of fact, even if matrix-fiber adhesion is stronger at lower kenaf contents, the presence of the compatibilizing agent allows to improve the matrix-fiber adhesion level, also at the highest amount of kenaf.

Mechanical analysis of neat PHBV and PHBV-based composites was performed at low (flexural) and high (impact) deformation rate to evaluate the influence of the fiber content and the compatibilization process on the stiffness and the toughness of prepared composites. Main mechanical results are reported in Table V.

Concerning the flexural properties, kenaf fibers significantly improve the Young modulus (E) up to 160% with respect to the PHBV value. This increase is a function of kenaf fiber content and interfacial adhesion

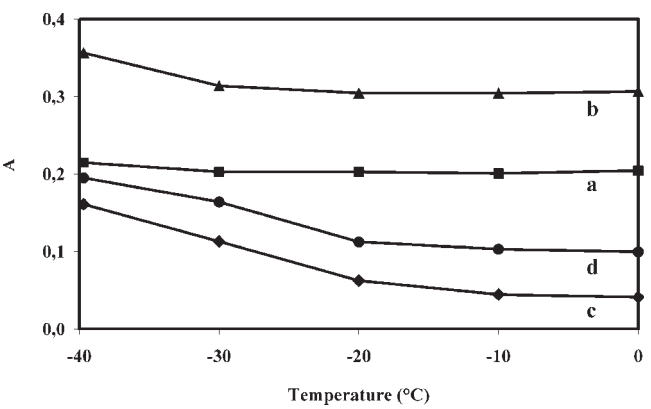

Figure 5 Adhesion parameter A for the samples: (a) PHBV/K 80/20; (b) PHBV/K 70/30; (c) PHBV/CA/K 75/5/20; (d) PHBV/CA/K 65/5/30.

TABLE V
Mechanical Analysis Results: Flexural and Impact Properties of Neat PHBV and PHBV Based Composites

	Flexural properties		Impact properties
Samples	Stress at maximum load (MPa)	Young's modulus (MPa)	Resilience (kJ/m^2)
PHBV neat	12.7	1067	2.72
PHBV/K 80/20	16.8	1812	3.28
PHBV/K 70/30	17.7	2214	3.46
PHBV/CA/K 75/5/20	16.9	2435	3.34
PHBV/CA/K 65/5/30	18.6	2788	3.88

strength. In fact, as described earlier, the decreasing of the A parameter signifies that matrix/fibers interactions occur. The relevance of these interactions is higher in the case of compatibilized with respect to uncompatibilized composites justifying a more pronounced improvement of the *E* value in the presence of CA. Moreover, the improvement of Young modulus is accompanied by the increase of flexural strength that represents a further evidence of the obtained matrix/fibers adhesion. These results can be well explained considering that kenaf fibers act as a reinforcement phase, representing critical area in which the applied load is concentrated. The extent of these phenomena is a function not only of the fiber content, but also of the matrix/fibers interfacial adhesion strength.

Nevertheless, the effect of the CA on these improvements seems to be more significant for Young's modulus than for stress at maximum load. This could be justified by considering the reactive nature of the CA used. In fact, reactions between MA groups grafted onto PHBV and kenaf fiber hydroxyl groups occur during the mixing, reducing the PHBV chain mobility. Such a reduced mobility is responsible for an increased stiffness of compatibilized composites, evidenced by the significant improvement of Young's modulus, but it also seems not to affect the stress transfer from the matrix to the fibers.

Finally, impact properties are also enhanced through the addition of kenaf fibers. In particular, the resilience of neat PHBV was increased by 21 and 27% for uncompatibilized composites containing 20% (PHBV/K 80/20) and 30% (PHBV/K 80/20) by weight of kenaf fibers, respectively. Concerning the compatibilized materials, a higher increase, up to 43%, was obtained by addition of 30 wt % of kenaf fibers (PHBV/CA/K 65/5/30).

Also for resilience, the improvement is a function of the fiber content and the compatibilization procedure. Moreover, comparing resilience results of uncompatibilized and compatibilized composites, a more pronounced difference is recorded for composites containing higher amount of fiber. In this case, the role of the compatibilizing agent is particularly significant, as also expected by the adhesion parameter analysis (Fig. 5), from which it has been already underlined that the gap of the adhesion parameter curves between compatibilized composites is about halved with respect to the extent of the gap between uncompatibilized composites, thus indicating again that the compatibilization procedure allows an increase of the matrix-fiber interfacial adhesion at high fiber contents.

CONCLUSIONS

A new class of biodegradable PHBV-based composites reinforced with kenaf fibers was prepared and characterized. Our approach based on the preparation of a proper compatibilizing agent has demonstrated that it is possible to improve the interfacial adhesion between the bacterial polyester PHBV and the kenaf fibers strongly enhancing the final properties of the composites. In particular, the main results of this work can be summarized as follows:

Compatibilized PHVB/kenaf composites show an improved adhesion between fibers and matrix, as confirmed both by morphological analysis and by the observation of the adhesion parameter curves.

Thermogravimetric analysis show that the chemical modification of PHBV does not influence the thermal and thermo-oxidative resistance of the prepared composites.

The compatibilization procedure induces significant improvements of the mechanical properties in comparison with neat PHBV.

References

1. Mohanty, A. K.; Misra, M.; Drzal, L. T. J Polym Environ 2002, 10, 19.
2. Mwaikambo, L. Y. In Low Environmental Impact Polymers; Tucker, N., Johnson, M., Eds.; Rapra Technology: Shawbury, UK, 2004; pp 1–24, .
3. Miller, M.; Barber, J.; Whitehouse, R. In Low Environmental Impact Polymers; Tucker, N., Johnson, M., Eds.; Rapra Technology: Shawbury, UK, 2004; pp 221–231.

4. Chen, G. G.-Q. In Biodegradable Polymers for Industrial Applications; Smith, R., Ed.; Woodhead: Cambridge, UK, 2005; pp 34–65.
5. Avella, M.; Errico, M. E. J Appl Polym Sci 2000, 77, 232.
6. Barham, P. J.; Keller, A.; Otun, E. L.; Holmes, P. A. J Mater Sci 1984, 19, 2781.
7. Shibata, M.; Takachiyo, K.-I.; Ozawa, K.; Yosomiya, R.; Takeishi, H. J Appl Polym Sci 2002, 85, 129.
8. Avella, M.; Casale, L.; Dell'Erba, R.; Focher, B.; Martuscelli, E.; Marzetti, A. J Appl Polym Sci 1997, 68, 1077.
9. Avella, M.; Casale, L.; Dell'Erba, R.; Martuscelli, E. Macromol Symp 1998, 127, 211.
10. Kaldor, A. F. Tappi J 1992, 10, 141.
11. Chen, H.-L.; Porter, R. S. J Appl Polym Sci 1994, 54, 1781.
12. Karnani, R.; Krishnan, M.; Narayan, R. Polym Eng Sci 1997, 37, 476.
13. Serizawa, S.; Inoue, K.; Iji, M. J Appl Polym Sci 2006, 100, 618.
14. Nishino, T.; Hirao, K.; Kotera, M.; Nakamae, K.; Inagaki, H. Compos Sci Technol 2003, 63, 1281.
15. Lee, S. G.; Choi, S.-S.; Park, W. H.; Cho, D. Macromol Symp 2003, 197, 89.
16. Flory, P. J. Principles of Polymer Chemistry; Cornell University Press: Ithaca, 1953.
17. Chan, C. H.; Kummerlowe, C.; Kammer, H.-W. Macromol Chem Phys 2004, 205, 664.
18. Scandola, M.; Focarete, M. L.; Adamus, G.; Sikorska, W.; Baranowska, I.; Swierczek, S.; Gnatowski, M.; Kowalczuk, M.; Jedlinski, Z. Macromolecules 1997, 30, 2568.
19. Martins, M. A.; Kiyohara, P. K.; Joekes, I. J Appl Polym Sci 2004, 94, 2333.
20. Hill, C. A. S.; Abdul Khalil, H. P. S. J Appl Polym Sci 2000, 78, 1685.
21. Avella, M.; Errico, M. E.; Rimedio, R.; Sadocco, P. J Appl Polym Sci 2002, 83, 1432.
22. Chen, C.; Zhou, X.; Zhuang, Y.; Dong, L. J Polym Sci Part B: Polym Phys 2005, 43, 35.
23. Chen, C.; Peng, S.; Fei, B.; Zhuang, Y.; Dong, L.; Feng, Z.; Chen, S.; Xia, H. J Appl Polym Sci 2003, 88, 659.
24. Assan, M. L.; Rowell, R. M.; Fadl, N. A.; Yacoub, S. F.; Christiansen, A. W. J Appl Polym Sci 2000, 76, 561.
25. Montaudo, G.; Puglisi, C.; Samperi, F. J Polym Sci Part A: Polym Chem 1994, 32, 15.
26. Montaudo, G.; Puglisi, C.; Samperi, F. Macromolecules 1998, 31, 650.
27. Porter, R. S.; Wang, L.-H. Polymer 1992, 33, 2019.
28. Hamilton, D. G.; Gallucci, R. R. J Appl Polym Sci 1993, 48, 2249.
29. Miley, D. M.; Runt, J. Polymer 1992, 33, 4643.
30. Mandelken, L. Crystallization of Polymers; McGraw-Hill: New York, 1964.
31. Avella, M.; Martuscelli, E.; Pascucci, B.; Raimo, M.; Focher, B.; Marzetti, A. J Appl Polym Sci 1993, 49, 2091.
32. Puglia, D.; Tomassucci, A.; Kenny, J. M. Polym Adv Technol 2003, 14, 749.
33. Avella, M.; Dell'Erba, R.; Martuscelli, E.; Partch, R. J Polym Mater 2000, 17, 445.
34. Avella, M.; Dell'Erba, R.; Focher, B.; Marzetti, A.; Martuscelli, E. Angew Makromol Chem 1995, 233, 149.
35. Kubat, J.; Rigdahl, M.; Welander, M. J Appl Polym Sci 1990, 39, 1527.